Current Topics in Peptide & Protein Research
Vol. 25, 2024

Original Article

Comparison of conventional versus ultra-high dose rate radiotherapy in MCF-7 and MCF-12A human breast cells: analysis of DNA damage response proteins

Marcin Zieliński[1,*], Aleksandra Lenartowicz-Gasik[2], Agnieszka Misiarz[2], Jacek Rzadkiewicz[3] and Janusz Kocik[4,5]

[1]NOMATEN Centre of Excellence, National Centre for Nuclear Research, Andrzeja Sołtana 7 Street, Otwock 05-400, Poland; [2]Nuclear Equipment Division, National Centre for Nuclear Research, Andrzeja Sołtana 7 Street, Otwock 05-400, Poland; [3]Nuclear Equipment and Technology Department, National Centre for Nuclear Research, Andrzeja Sołtana 7 Street, Otwock 05-400, Poland; [4]Radiological Metrology and Biomedical Physics Division, National Centre for Nuclear Research, Andrzeja Sołtana 7 Street, Otwock 05-400, Poland; [5]Department of Cancer and Infectious Diseases, Centre of Postgraduate Medical Education, Marymoncka 99/103 Street, Warsaw 01-813, Poland.

ABSTRACT

Radiotherapy (RT) is one of the most important treatment modalities for the cure of cancer. Around 50% of cancer patients are treated with RT alone or in combination with other treatment modalities, such as chemotherapy. However, in the treatment of radioresistant tumors the total radiation dose that can be delivered to the tumor is often limited by the radiation tolerance of neighboring, critical, normal tissues. In such situations, ultra-high dose rate (UHDR-RT) could be of significant interest. Compared with conventional radiotherapy, UHDR-RT can effectively reduce the toxicity in normal tissues and provide similar antitumor effects, which is defined as the FLASH effect. The biological mechanisms responsible for the reduction of normal tissue toxicities with FLASH irradiation compared to CONV are not fully understood. In FLASH, the intrinsic factors "DNA damage" or "clustered DNA damage" is likely involved in the differential response between healthy and tumor tissue. In this paper we show our preliminary study results in which it was planned to investigate the response of selected cell lines MCF-7 and MCF-12A to DNA damage at the protein level, and to doses of ionizing radiation typical for conventional and ultra-high radiotherapy. The cells were exposed to electron beam irradiation at two different dose rates: 0,0833 Gy/s and 10 Gy/s. After irradiation, at various time intervals the cells were lysed and lysates were analyzed by Western blot method with a set of antibodies directed against several important proteins involved in the repair of DNA double-strand breaks and designed to characterize the phosphorylation state of the kinases ATM and DNA-PKcs reacting to DNA damage, and proteins used for assessment of apoptosis induction. Our preliminary results showed some differences in biological response, both between the dose rates used (CONV versus UHDR) and between MCF-7 cancer cells and healthy MCF-12A cells.

KEYWORDS: radiobiology, conventional radiotherapy, ultra-high dose radiotherapy, electron beam, breast cancer, biological response, proteomic research.

INTRODUCTION

Radiotherapy (RT) is one of the most important treatment modalities for the cure and palliation of

*Corresponding author: marcin.zielinski@ncbj.gov.pl

cancer. Around 50% of cancer patients are treated with RT alone or in combination with other treatment modalities, such as chemotherapy [1]. The essence of RT is effectively killing tumor cells with minimal exposure of the neighboring healthy tissues. Over the past decades, advances in technology have improved precision delivery of radiation with high conformity to the target. With conventional radiotherapy (CONV-RT) discrimination between tumor and normal tissue responses is achieved by the tissue-sparing effect of dose fractionation, allowing healthy tissues to recover to a greater extent than the tumor [2]. However, in the treatment of radioresistant tumors the total radiation dose that can be delivered to the tumor is often limited by the radiation tolerance of neighboring, critical, normal tissues. In such situations, ultra-high dose rate (UHDR-RT) could be of significant interest. Compared with conventional radiotherapy, UHDR-RT can effectively reduce the toxicity in normal tissues and provide similar antitumor effects, which is defined as the FLASH effect [3]. The biological mechanisms responsible for the reduction of normal tissue toxicities with FLASH irradiation compared to CONV are not fully understood. Several hypotheses have been proposed to explain the biological mechanisms contributing to the selective FLASH effect, including differences between healthy and cancer cells in the production of reactive oxygen species and free radicals, limitation of Fenton reaction caused by high $Fe^{2+/3+}$ levels in tumor cells, and impaired DNA damage repair mechanisms occurring in cancer [4]. The classic target theory considers DNA as the major target of ionizing radiation. As a lethal effect of radiation, unrepaired DNA double strand breaks (DSBs) are considered to determine the fate of the cell. In FLASH, the intrinsic factors "DNA damage" or "clustered DNA damage" is likely involved in the differential response between healthy and tumor tissue [2]. In this paper we show our preliminary study results in which it was planned to investigate the response of selected cell lines MCF-7 and MCF-12A to DNA damage at the protein level, and to doses of ionizing radiation typical for conventional and ultra-high radiotherapy. Breast cancer MCF-7 cell line (ATCC HTB-22) and healthy breast MCF-12A cell line (ATCC CRL-10782) were exposed to electron beam irradiation at two different dose rates: 0,0833 Gy/s and 10 Gy/s. After irradiation, at various time intervals the cells were lysed and lysates were analyzed by Western blot method with a set of antibodies directed against several important proteins involved in the repair of DNA double-strand breaks and designed to validate and characterize the phosphorylation state of the kinases ATM and DNA-PKcs reacting to DNA damage, and proteins used for quick assessment of cell cycle distribution and apoptosis induction based on molecular markers of the G1/S and M phases of the cell cycle and the presence of the digested PARP enzyme. We report here the outcome of these experiments.

MATERIALS AND METHODS

Cell culture

The human breast cancer and normal cell lines, MCF-7 and MCF-12A respectively, were donated from The Greater Poland Cancer Centre. MCF-7 cells were maintained in Dulbecco's Modified Eagle Medium (DMEM) (Gibco, Thermo Fisher Scientific) with high glucose (4.5 g/l), sodium pyruvate and glutamine supplemented with 10% fetal bovine serum (FBS, Gibco, Thermo Fisher Scientific), 1% penicillin/streptomycin (Gibco, Thermo Fisher Scientific) and 0.01 mg/ml human insulin (Gensulin R, Bioton S.A.) at 37 °C in a humidified atmosphere of 5% CO_2. MCF-12A cells were maintained in Dulbecco's Modified Eagle Medium:Nutrient Mixture F-12 (DMEM / F-12) (Gibco, Thermo Fisher Scientific) supplemented with 5% horse serum (Gibco, Thermo Fisher Scientific), 1% penicillin/streptomycin (Gibco, Thermo Fisher Scientific), 0.01 mg/ml human insulin (Gensulin R, Bioton S.A.), 0.02 μg/ml human epidermal growth factor (Gibco, Thermo Fisher Scientific), 0.5 μg/ml hydrocortisone (Sigma-Aldrich, Merck) and 0.1 μg/ml Cholera toxin (Sigma-Aldrich, Merck) at 37 °C in a humidified atmosphere of 5% CO_2 and 95% air. 1 x 10^6 cells from each cell lines (MCF-7 and MCF-12A) were seeded in T-25 cell culture flasks (Googlab Scientific) and left in CO_2 incubator (NU-5710E model, NuAire).

Chemical induction of hypoxia – preparation of $CoCl_2$ stock solution and hypoxia treatment

Stock solution (25 mM) of cobalt chloride ($CoCl_2$) (Cobalt(II) chloride hexahydrate, Sigma-Aldrich)

was prepared in sterile distilled water and further diluted in medium in order to obtain the final desired concentration. MCF-7 and MCF-12A cell lines were treated with 100 μM concentration of $CoCl_2$ and incubated under CO_2 incubator for 24 hours before irradiation.

Irradiation and dosimetry

Irradiations were performed using intraoperative radiotherapy (IORT) linear accelerator designed and manufactured in collaboration with the Greater Poland Cancer Centre in an EU project. The device is available at the National Centre for Nuclear Research (Otwock, Poland). In this device two modes are available: with conventional intraoperative radiotherapy dose rates (5 and 10 Gy/min.) and with ultra-high doses (higher dose rate than conventional dose rates). The conventional intraoperative mode can generate a beam with energies from 4 to 12 MeV. In this study, using conventional mode cell culture flasks were irradiated by a 6 MeV electron beam with 5 Gy/min. dose rate. Before irradiation dose rates in conventional mode were measured using typical electron beam detector - Markus Advance chamber (type 34045 PTW Freiburg, Germany). Doses delivered to cells flask were 2.45 ± 0.02 Gy. The beam quality parameters obtained for the conventional 6 MeV beam were in accordance with the requirements of the International Electrotechnical Commission (IEC). The accelerator was upgraded to generate high dose rate mode, where dose rates were higher than conventional dose rates for two beam energies of 6 and 9 MeV (measured used film dosimetry for source to surface distance (SSD) of 60 cm and a circular field diameter of 10 cm). In ultra-high dose rate mode irradiations of cell culture flasks were made with higher dose rate of 6 MeV beam and 10 Gy/s dose rate and were performed by a program that allows to generate single pulse of irradiation. In the higher dose rate mode, all measurements were performed using passive dosimetry - radiochromic film dosimetry (Gafchromic EBT-XD films). During irradiation radiochromic films were placed under the cell to measure dose. Three of the films used during the irradiation of biological material are presented in Figure 1. Before irradiation, a correction factor was determined and applied to the attenuation of the beam after passing through the medium and the bottom of the cell. Radiochromic films were scanned 24 hours after irradiation using a Perfection V850 Pro flatbed scanner (Epson, Long Beach, CA, USA) at 72 dpi resolution. After that films were analyzed using a calibration curve prepared for a 9 MeV electron beam using 15 film Gafchromic EBT-XD pieces (shown on Figure 2), irradiated on SSD = 60 cm with field size of 10 cm in diameter, made using medical accelerator. The results showed that the cells were irradiated by a 6 MeV beam in a higher dose rate mode (10 Gy/s) that delivered a dose of 2.35 ± 0.11 Gy.

Cell lysis and protein extraction for Western blotting

At several time points after cell irradiation (15 min., 30 min., 1 h, 3 h, 6 h, 24 h, 48 h, 72 h) cells were

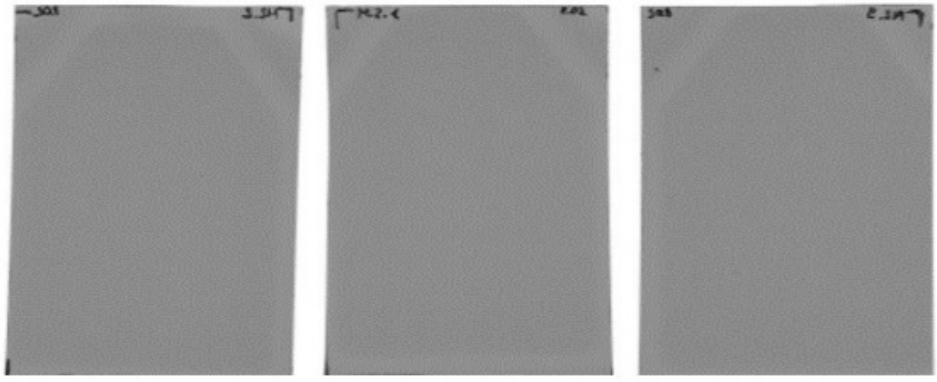

Figure 1. Gafchromic EBT-XD films used during the irradiation of the biological material.

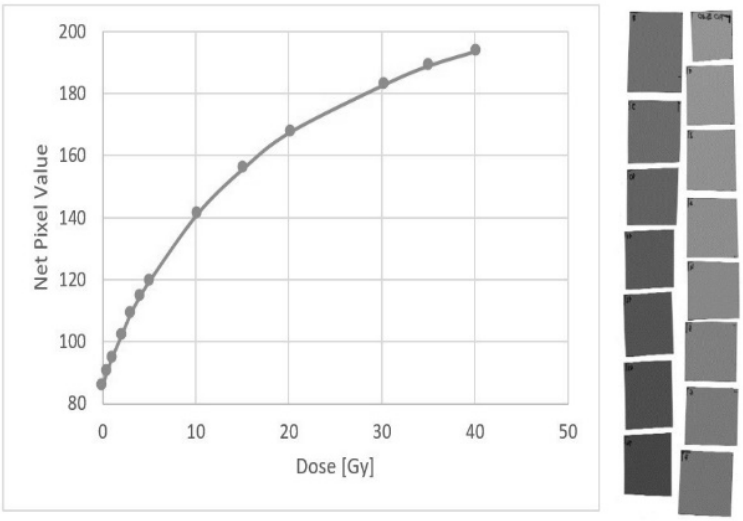

Figure 2. Film dosimetry calibration curve and 15 calibration film pieces of Gafchromic EBT-XD.

washed twice in PBS pH 7.4 and trypsinized with trypsin-EDTA (0.25 %) solution (Gibco, Thermo Scientific) and then centrifuged (5 min., 200 x g). After centrifugation the supernatant was discarded and tubes with the pellet fraction were put on ice without pellet resuspension. Then the cells were lysed in RIPA lysis and extraction buffer (Thermo Scientific). To protect proteins from degradation during extraction the Halt Protease and Phosphatase Inhibitor Cocktail (Thermo Scientific) was added to lysis buffer. The lysates were kept on ice for 30 minutes with the RIPA buffer, and soluble proteins recovered after centrifugation (20 000 x g for 15 min.) were quantified by Bradford assay and analyzed by Western blot. Additionally, lysates from MCF-7 and MCF-12A cells not subjected to irradiation were prepared in the same way as a negative control.

Western blot analysis

Non-homologous end joining (NHEJ) antibody panel (ab213658, Abcam), DNA damage kinases panel (ab103970, Abcam) and cell cycle and apoptosis WB cocktail (ab139417, Abcam) were used for analyses. Non-homologous end joining panel is designed for the detection and characterization of key proteins involved in DNA double strand break (DSB) repair by NHEJ. Histone H2A.X is phosphorylated on S139, termed gamma H2A.X, at sites of DNA damage. DNA DSB repair by NHEJ requires Ku70/Ku80 heterodimer binding to the DSB, as well as DNA Ligase IV for ligation of DNA ends. This panel contains 5 recombinant rabbit monoclonal antibodies: rabbit monoclonal anti-Histone H2A.X antibody [EPR895], rabbit monoclonal anti-gamma H2A.X (phospho S139) antibody [EP854(2)Y], rabbit monoclonal anti-DNA Ligase IV/LIG4 antibody [EPR16531], rabbit monoclonal anti-Ku70 antibody [EPR4027] and rabbit monoclonal anti-Ku80 antibody [EPR3468]. DNA damage kinases panel is designed for the validation and characterization of the phosphorylation state of the DNA damage responsive kinases ATM and DNA-PKcs. ATM and DNA-PK are protein kinases that are active and become phosphorylated in response to DNA double strand breaks (DSBs). ATM is phosphorylated on S1981 and is involved in phosphorylation of various proteins during the cellular response to DNA DSBs, while DNA-PK, a key component of the non-homologous end-joining pathway of DSB repair, is phosphorylated on S2056. The panel contains: anti-ATM antibody [EPR17059], anti-ATM (phospho S1981) antibody [EP1890Y], anti-ATR antibody, anti-ATR (phospho S428) antibody, anti-DNA PKcs antibody [Y393] and anti-DNA PKcs (phospho S2056) antibody [EPR5670]. The cell cycle and apoptosis Western blot cocktail (ab139417) is designed to provide a rapid assessment of cell cycle distribution and apoptosis induction based on molecular markers for the G1/S and M phases of the cell cycle and the

presence of cleaved PARP. This is a mixture of four highly specific monoclonal primary antibodies targeting Cdk2 pTyr15, Histone H3 pSer10, cleaved-PARP and Actin. Cyclin-dependent kinase 2 (Cdk2) is maintained in an inactive state in G1/S by inhibitory phosphorylation on Tyr15. Histone H3 is phosphorylated at Ser10 when chromosomes condense during mitosis. Hence, elevated Cdk2 pTyr15 indicates G1/S arrested cells and elevated Histone H3 pSer10 indicates M-phase arrested cells when compared to asynchronous cycling control cells. Poly [ADP-ribose] polymerase 1 (PARP) is a DNA repair enzyme that is cleaved by activated caspases, and hence cleaved-PARP indicates induction of apoptosis. In our studies we used not all, but selected antibodies from individual kits. The protein samples were denatured in Laemmli sample buffer, boiled for 5 min. at 100 °C, and analyzed by Western blot. 50 µg of protein was loaded into each well and separated by sodium dodecyl sulphate-polyacrylamide gel electrophoresis (SDS-PAGE) followed by transfer to polyvinylidene fluoride (PVDF) (Bio-Rad). Consequently, after the blocking step primary antibody for each protein like Cdk2 pTyr15[1], Histone H3 pSer10[1], cleaved-PARP[1], Actin[1], anti-gamma H2A.X (phospho S139)[2], anti-DNA PKcs (phospho S2056)[3], anti-ATR[4], anti-Ku70[5], anti-Ku80[6], anti-DNA ligase IV[7] (numbers 1-7 correspond to dilution of specified antibodies) was added in blocking solution (5% BSA/PBS+0.05%Tween 20) with dilution: 1-(1:250), 2-(1:5000), 3-(1:7500), 4-(1:2500), 5-(1:2500), 6-(1:2500) and 7-(1:1000) and incubated for 16-18 h at 4 °C. The membrane was washed five times in TBST and then incubated for 2 h with secondary antibody (Goat anti-rabbit IgG H&L HRP) (ab205718, Abcam) (secondary antibodies have been used with 1:20,000 dilution). Subsequently the membrane was washed five times in TBST and exposed to X-ray film (CL-Xposure film, Thermo Scientific). The expression of proteins was detected and captured.

RESULTS

To compare the cellular response to conventional and ultra-high dose rate radiotherapy, we used human breast cancer MCF-7 and normal breast MCF-12A cells. We have also conducted previous research with human breast cancer cells on preparing an electron accelerator for radiobiological research [5]. Since it has been show that the FLASH effect of ultra-high dose rate radiotherapy depends on oxygen concentration [6] we cultured selected cell lines under chemically induced hypoxia. So we had two groups of cells to irradiate: 1) MCF-7 and MCF-12A / chemically induced hypoxia / conventional dose rate, 2) MCF-7 and MCF-12A / chemically induced hypoxia / ultra-high dose rate. Cells were treated with a single fraction of about 2.5 Gy electron radiation delivered using 2 different modalities: (1) conventional dose rate delivering 5 Gy/min. (0,0833 Gy/s) and (2) ultra-high dose rate delivering 10 Gy/s. Appropriate controls were unirradiated cells (MCF-7 and MCF-12A) cultured under chemically induced hypoxic conditions. Cells were detached and cell lysates were prepared at 15 minutes, 30 minutes, and 1, 3, 6, 12, 24, 48, and 72 hours after irradiation. Proteins involved in the repair of DNA double-strand breaks (DSBs) through the non-homologous end joining (NHEJ) mechanism (histone gamma H2A.X phospho S139, DNA ligase IV, Ku 70 and Ku 80), DNA kinase-PKcs, cyclin-dependent kinase 2 (pTyr15), histone H3 pSer10, and cleaved-PARP expression were assessed across normal and cancerous human breast cell lines. The results of Western blot analysis are shown in Figures 3-9.

γ – H2A.X (phospho S139)

Under UHDR conditions, histone H2A.X gamma protein bands are visible in all samples in MCF-7 cells, but there is no signal from lysate samples derived from MCF-12A cells. In conventional conditions, a weak signal is visible after 24 and 48 hours and a stronger signal is visible 72 hours after irradiation in MCF-7 cells. There are no signals in samples from MCF-12A cells.

DNA ligase IV

There is no visible DNA ligase IV protein expression in both cell lines exposed to conventional radiotherapy conditions. In the case of UHDR therapy, double bands are visible, the intensity of which increases with time after irradiation.

Ku 70

For UHDR radiotherapy conditions a low intensity band can be observed in MCF-7 cells

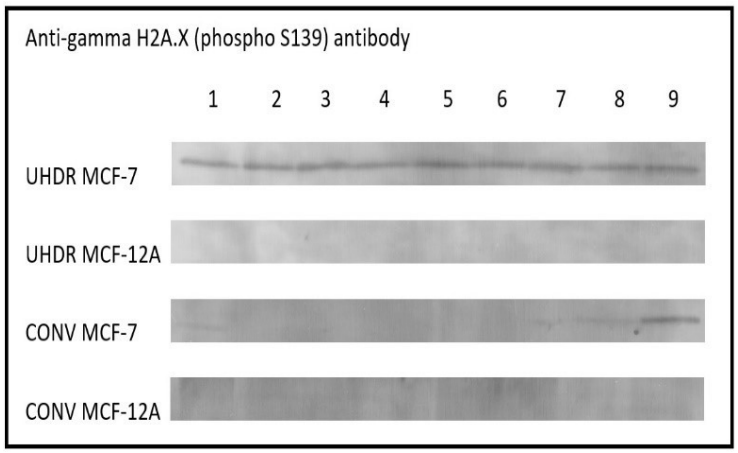

Figure 3. Western blot analysis for the expression of gamma H2A.X (phosphor S139) in MCF-7 and MCF-12A cells treated with conventional dose rate (CONV) and ultra-high dose rate (UHDR). Lanes: 1 – non-irradiated cells, 2 – 15 min., 3 – 30 min., 4 – 1 hour, 5 – 3 hours, 6 – 6 hours, 7 – 24 hours, 8 – 48 hours, 9 – 72 hours after exposure.

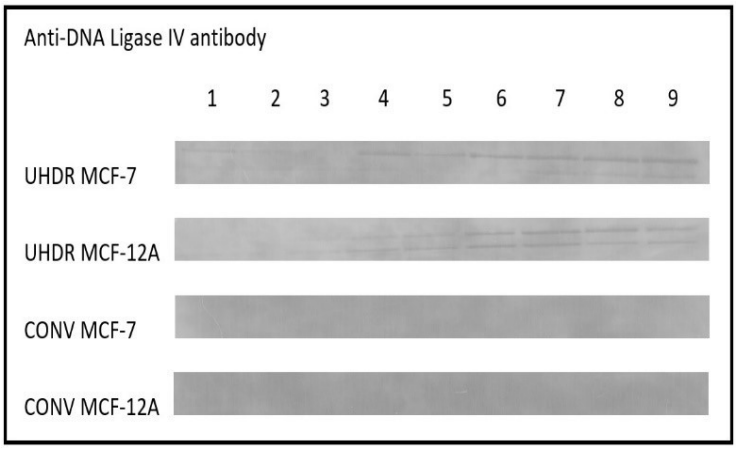

Figure 4. Western blot analysis for the expression of DNA ligase IV in MCF-7 and MCF-12A cells treated with conventional dose rate (CONV) and ultra-high dose rate (UHDR). Lanes: 1 – non-irradiated cells, 2 – 15 min., 3 – 30 min., 4 – 1 hour, 5 – 3 hours, 6 – 6 hours, 7 – 24 hours, 8 – 48 hours, 9 – 72 hours after exposure.

1 hour after irradiation, the intensity of which increases with time. In MCF-12A cells double bands are visible in all lanes which are more intense from the 6th hour after irradiation. There is no visible Ku 70 protein expression in both cell lines exposed to conventional radiotherapy conditions, except for a weak band in the unirradiated MCF-7 cell sample.

Ku 80

As for the Ku 80 protein, in cells subjected to UHDR radiotherapy conditions, expression is visible in all samples in both cell lines but in MCF-7 there is strong expression, and in MCF-12A it is visible that the intensity of the bands increases with time. Under conventional radiotherapy conditions, Ku 80 protein expression is visible only in MCF-7 cells.

DNA PKcs (phospho S2056)

For UHDR-RT conditions very low intensity bands are visible from 30 minutes to 24 hours after irradiation in MCF-7 cell line and there are

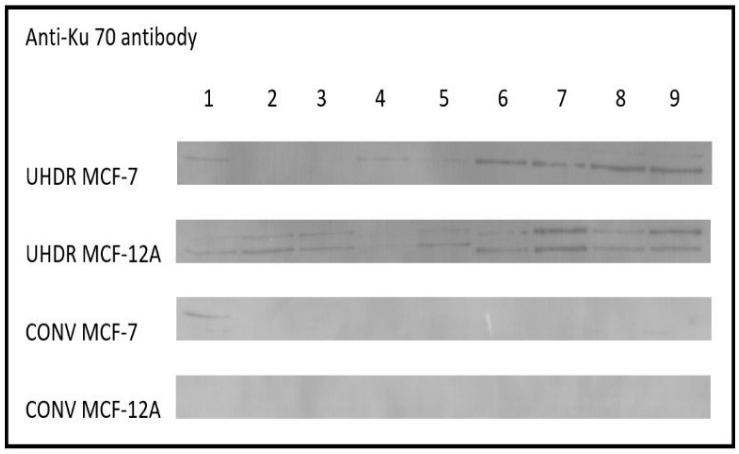

Figure 5. Western blot analysis for the expression of Ku 70 in MCF-7 and MCF-12A cells treated with conventional dose rate (CONV) and ultra-high dose rate (UHDR). Lanes: 1 – non-irradiated cells, 2 – 15 min., 3 – 30 min., 4 – 1 hour, 5 – 3 hours, 6 – 6 hours, 7 – 24 hours, 8 – 48 hours, 9 – 72 hours after exposure.

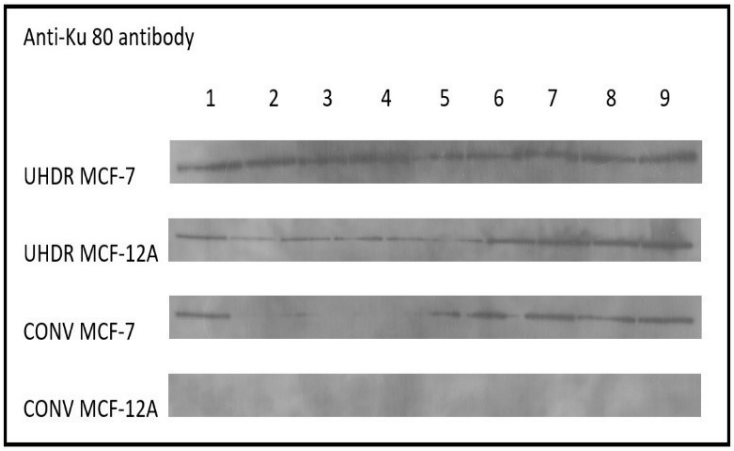

Figure 6. Western blot analysis for the expression of Ku 80 in MCF-7 and MCF-12A cells treated with conventional dose rate (CONV) and ultra-high dose rate (UHDR). Lanes: 1 – non-irradiated cells, 2 – 15 min., 3 – 30 min., 4 – 1 hour, 5 – 3 hours, 6 – 6 hours, 7 – 24 hours, 8 – 48 hours, 9 – 72 hours after exposure.

no bands in MCF-12A cells. In conventional radiotherapy mode we obtained some non-specific binding and multiple bands (data not shown).

Cell cycle and apoptosis Western blot cocktail (Cdk2 pTyr15, Histone H3 pSer10, cleaved-PARP, Actin)

In the case of UHDR, the presence of histone H3 pSer10 protein is visible at all time points after irradiation in MCF-7 cells. However, there is no expression in MCF-12A cells except in a sample taken 6 hours after irradiation. Under conventional conditions, both cell lines express the histone H3 pSer10 protein - in all samples in the MCF-7 line and up to 6 hours after irradiation in the MCF-12A line. There were no signals from the Cdk2 pTyr15 and cleaved-PARP proteins (data not shown). Actin was used as a loading control.

DISCUSSION

In recent years, ultra-high dose rate radiotherapy (UHDR-RT) has gained attention in preclinical studies as a potential advancement in cancer treatment. The great advantage of UHDR-RT is

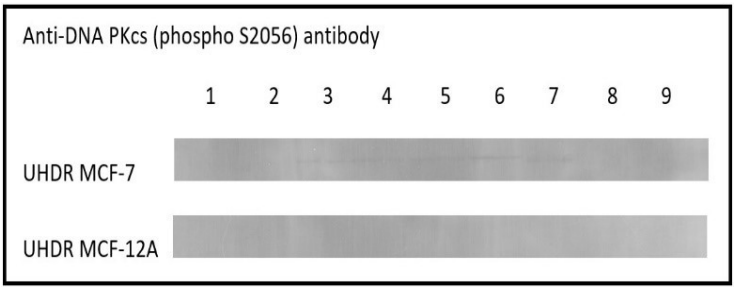

Figure 7. Western blot analysis for the expression of DNA PKcs (phospho S2056) in MCF-7 and MCF-12A cells treated with conventional dose rate (CONV) and ultra-high dose rate (UHDR). Lanes: 1 – non-irradiated cells, 2 – 15 min., 3 – 30 min., 4 – 1 hour, 5 – 3 hours, 6 – 6 hours, 7 – 24 hours, 8 – 48 hours, 9 – 72 hours after exposure.

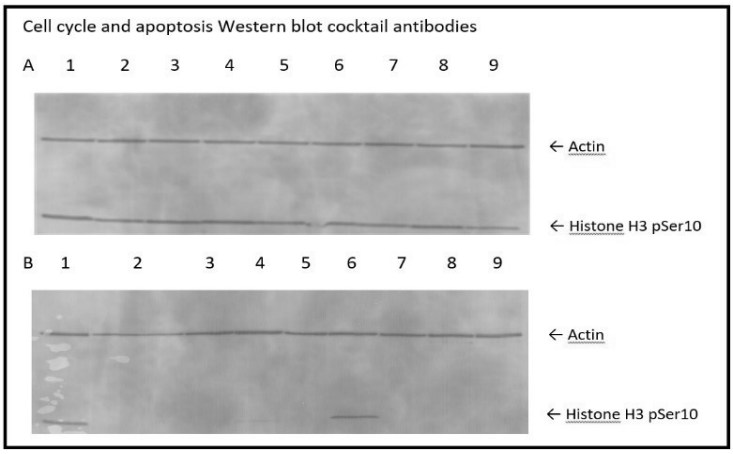

Figure 8. Western blot analysis for the expression of proteins used to assess cell cycle distribution and apoptosis induction based on molecular markers of the G1/S and M phases of the cell cycle and the presence of the cleaved PARP enzyme in MCF-7 (A) and MCF-12A (B) cells treated with ultra-high dose rate (UHDR). Lanes: 1 – non-irradiated cells, 2 – 15 min., 3 – 30 min., 4 – 1 hour, 5 – 3 hours, 6 – 6 hours, 7 – 24 hours, 8 – 48 hours, 9 – 72 hours after exposure.

the ultra-fast, high dose delivery that has a similar or greater effect to cancer cells while sparing normal, healthy tissue surrounding the tumor site. Several hypotheses have been proposed to explain the biological mechanisms contributing to the selective FLASH effect, including differences between healthy and cancer cells in the production of reactive oxygen species and free radicals, limitation of Fenton reaction caused by high $Fe^{2+/3+}$ levels in tumor cells, and impaired DNA damage repair mechanisms occurring in cancer [6]. It was shown that a mechanism depending on differences in the extent and type of DNA damage resulting from FLASH- versus CONV-RT could contribute to the observed FLASH effect. The highly energetic ionizing radiation used in RT is what kills tumors. Specifically, the energy of this type of radiation induces double-stranded DNA breaks that overwhelm DNA repair mechanisms, leading to cell death. FLASH- and CONV-RT seem to cause different types of DNA damage in normal tissues and tumors [7]. Therefore, we wanted to examine the expression level of proteins involved in the repair of DNA damages. We used chemically induced hypoxia method with a cobalt chloride solution ($CoCl_2$) which is a commonly used hypoxia-mimetic agent that artificially induces hypoxia and can block the

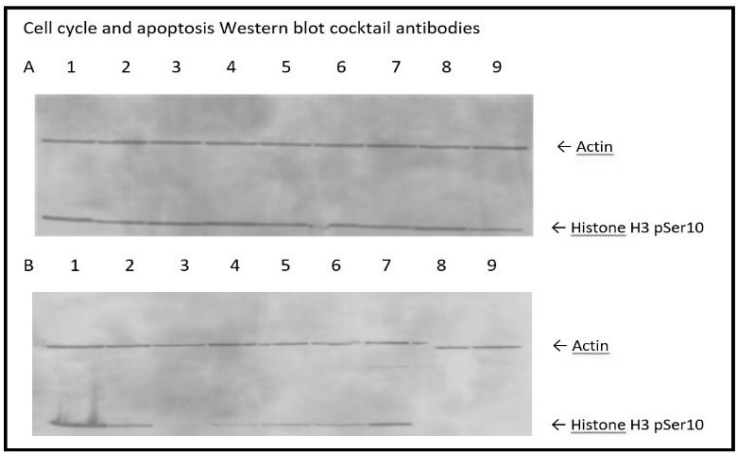

Figure 9. Western blot analysis for the expression of proteins used to assess cell cycle distribution and apoptosis induction based on molecular markers of the G1/S and M phases of the cell cycle and the presence of the cleaved PARP enzyme in MCF-7 (A) and MCF-12A (B) cells treated with conventional dose rate (CONV). Lanes: 1 – non-irradiated cells, 2 – 15 min., 3 – 30 min., 4 – 1 hour, 5 – 3 hours, 6 – 6 hours, 7 – 24 hours, 8 – 48 hours, 9 – 72 hours after exposure.

degradation and thus induces the accumulation of HIF-1α protein [8]. Our preliminary results showed some differences in biological response, both between the dose rates used (CONV versus UHDR) and between MCF-7 cancer cells and healthy MCF-12A cells (Table 1).

Activation of histone gamma H2A.X, DNA ligase IV, Ku 70 and Ku 80 protein complex and slight DNA PKcs activity can be seen in MCF-7 cells subjected to UHDR radiotherapy conditions. On the other hand, the response of MCF-12A cells to radiation appears to be delayed or weaker. Ku 70 and Ku 80 proteins and DNA ligase IV are present, but there is no activation of histone gamma H2A.X and DNA kinase-PKcs under UHDR conditions. Additionally, in both MCF-7 and MCF-12A cells there was no activation of the apoptosis process (no Cdk2 pTyr15 and cleaved-PARP proteins bands). Only histone H3 pSer10 phosphorylation is visible in cancer MCF-7 under conventional radiation dose rate, which indicates that M-phase arrested cells when compared to asynchronous cycling control cells.

The H2A histone family member X (H2AX) is a variant of the histone protein H2A. It is involved in nucleosome formation and chromatin remodeling and is an essential protein for DNA DSB repair [9]. DNA DSB repair is a very important biological mechanism that recognizes and corrects damage or abnormalities in genome. H2A.X phosphorylation has a key role in the repair process. The two major pathways for DNA DSB repair are homologous recombination (HR) and nonhomologous end-joining (NHEJ). The

first leads to accurate repair, while the second can be mutagenic – both involve γH2A.X [10, 11]. For its early involvement, γH2A.X is considered a marker of very-early response to DSBs. Immunofluorescence analysis showed that γH2A.X foci are detectable at the sites of DSBs within 3 minutes after DNA damage stimulation and continue to increase until a plateau is achieved in 10–30 minutes, where the number of γH2A.X foci has been shown to correlate with the number of DSBs [12]. Then, a kinetic disappearance is observed up to about 24 h, where γH2A.X levels return approximatively to baseline. We were surprised with the presence of the histone gamma H2AX band in MCF-7 cells not exposed to radiation (Figure 3 – lane 1). It has been shown that, in untreated normal and tumor cells, a fraction of the histone H2A.X remain phosphorylated and the extent of this constitutive H2A.X phosphorylation depends on cell type and cell-cycle phase [13, 14, 15, 16]. While in interphase H2A.X phosphorylation reflects a DNA-damage response involving the presence of DSBs, these events in mitotic cells may also be associated with

Table 1. Pooled Western blot results ("0" – no expression; "+" – expression of protein of interest).

Protein \ Cell line and irradiation conditions	Cancer MCF-7 Conv-RT	Non-cancer MCF -12A Conv-RT	Cancer MCF-7 UHDR-RT	Non-cancer MCF-12A UHDR-RT
Gamma H2A.X	+	0	+	0
Ligase IV	0	0	+	+
Ku 70	0	0	+	+
Ku 80	+	0	+	+
DNA kinase-PKcs	0	0	+	0
Histone H3 pSer10 (M-phase arrested cells)	+	+	+	0
Cdk2 pTyr15 and cleaved-PARP proteins (Apoptosis)	0	0	0	0

catalytic torsional stress following chromatin condensation that may represent the signal triggering H2A.X phosphorylation even in the absence of DSBs [16, 17, 18]. As for the Ku 70 and Ku 80 proteins, the resulting heterodimer Ku70/80 is a central actor of the c-NHEJ pathway. It is considered as one of the first factors to be recruited at DSB sites because of its high affinity for DNA ends (Kd in the nM range) and its high abundance in the nucleus [19]. Via its C-terminal region, Ku interacts with the DNA-dependent protein kinase catalytic subunit (DNA-PKcs) to form the DNA-PK holoenzyme, which controls the interaction between broken DNA ends during c-NHEJ [20, 21, 22].

Once DNA double strand breaks (DSBs) occur in the cells, DNA-PKcs is promptly recruited into damage sites and activated, participating in a wide multi-faceted series of repair processes, which determine the cells' fates: DSBs NHEJ repair and pathway choice, replication stress response, cell cycle checkpoints, telomeres length maintenance, senescence, autophagy, etc. Combining DNA-PKcs inhibitors with radiotherapy can effectively enhance the efficacy of radiotherapy.

In our study the singular dose of 2,45 ± 0,015 Gy at conventional radiotherapy dose rate was not able to elicit expression/activation of histone gamma H2A.X, DNA ligase IV, Ku 70/80 and DNA PKcs, in healthy MCF-12A cells. In cancer MCF-7 cells the only sign of DNA damage caused by radiation was a late signal (72 hours after irradiation) of histone H2A.X phosphorylation and increasing expression of the Ku 80 protein (only one part of the Ku 70/80 heterodimer) that is capable of activating downstream proteins in NHEJ repair. This gentle biological response to the radiation trigger might not only be an aftermath of DNA DSB but also due to H2A.X phosphorylation production in the absence of DSBs, caused by other cellular processes. Both cell lines had been arrested in mitosis phase but did not undergo apoptosis. What is interesting and surprising is that ultra-high dose electron beam of 10 Gy/s with the delivered singular dose of 2.35 ± 0.11 Gy was able to elicit different profiles of DNA damage in cancer and normal cells. Gamma H2A.X and DNA kinase-PKcs were not prompted in normal cells and they were not arrested in mitosis. The response to DNA damage in cancer cells under UHDR radiotherapy conditions seems to be stronger - Ku70 and Ku80 proteins and other proteins from the NHEJ repair pathway (Ligase IV and DNA kinase-PKcs) were activated. Those last catalytic subunits were not expressed in normal cells. This may indicate low burden of dsDNA breaks in normal cells. Those cells were also not arrested in cell cycle. Even though the cancer cells were arrested in mitosis there are no proteins indicating the initiation of the apoptosis process. A limitation of our study is the dose rate used (10 Gy/s) instead 40 Gy/s as for FLASH radiotherapy. Perhaps it is why the expression of DNA damage-related proteins is equivocal.

CONCLUSION AND FUTURE PERSPECTIVES

In summary, we will definitely continue our research with a beam with a dose rate of at least 40 Gy/s. We will also change the research model and instead of 2D cell cultures we will use 3D spheroids. 2D cultured cells do not mimic the natural structures of tissues or tumours. In this culture method, cell-cell and cell-extracellular environment interactions are not represented as they would be in the tumour mass. The concept of 3D spheres is based on the creation of spheroid structures in which cells form various layers. This structure mimics the physical and biochemical features of a solid tumour mass [23]. We will also want to replace the chemiluminescence-based western blotting method with a fluorescence-based method to precisely determine the amount of individual proteins. Fluorophore signal more linearly correlates with protein concentration, likely because it is a more direct assessment of protein abundance than enzymatic function in chemiluminescent method. It also provides a greater dynamic range, offering superior sensitivity for both low and high protein amounts [24, 25].

ACKNOWLEDGEMENTS

The Author(s) were supported [partially - if appropriate] by the European Union Horizon 2020 research and innovation program under Grant Agreement No. 857470 and from the European Regional Development Fund under the program of the Foundation for Polish Science International Research Agenda PLUS, grant No. MAB PLUS/2018/8, and the initiative of the Ministry of Science and Higher Education ‘Support for the activities of Centers of Excellence established in Poland under the Horizon 2020 program’ under agreement No. MEiN/2023/DIR/3795.

FUNDING

This work was supported by National Science Centre (NCN) Grant Number 2021/05/X/NZ5/00425.

AUTHOR CONTRIBUTIONS

Marcin Zieliński: Conceptualization, Methodology, Investigation, Resources, Writing – Original draft preparation, Project administration, Funding acquisition; **Aleksandra Lenartowicz-Gasik:** Conceptualization, Methodology, Investigation, Writing – Original draft preparation; **Agnieszka Misiarz:** Methodology, Writing – Reviewing and Editing; **Jacek Rzadkiewicz:** Validation, Writing – Reviewing and Editing, Supervision; **Janusz Kocik:** Conceptualization, Writing – Reviewing and Editing, Supervision

CONFLICT OF INTEREST STATEMENT

The authors declare that they have no known competing financial interests or personal relationships that could have appeared to influence the work reported in this paper.

REFERENCES

1. Yap, M. L., Zubizarreta, E., Bray, F., Ferlay, J. and Barton, M. 2016, Journal of Global Oncology, 2, 207–215.
2. Zhou, G. 2020, Radiation Medicine and Protection, 1, 35–40.
3. Favaudon, V., Labarbe, R. and Limoli, C. L. 2022, Medical Physics, 49(3), 2068–81.
4. Del Debbio, F., Bertilacchi, M. S., Gonnelli, A., Da Pozzo, E., Tozzini, V., Martini, C., Capaccioli, S. and Costa, B. 2023, Frontiers in Physics, 11, 1201708. doi: 10.3389/fphy.2023.1201708
5. Dróżdż, A., Waluś, M., Zieliński, M., Malesa, B., Kruszyna-Mochalska, M., Kulcenty, K., Adamczyk, B., Nowaczyk, P., Malicki, J. and Pracz, J. 2021, Reports of Practical Oncology and Radiotherapy, 26(6), 1029-1034.
6. Adrian, G., Konradsson, E., Lempart, M., Bäck, S., Ceberg, C. and Petersson, K. 2020, British Journal of Radiology, 93, 20190702.
7. Prempree, T., Michelsen, A. and Merz, T. 1969, International Journal of Radiation Biology and Related Studies in Physics, Chemistry, and Medicine, 15, 571–574.
8. Huang, Y., Du, K-M., Xue, Z-H., Yan, H., Li, D., Liu, W., Chen, Z., Zhao, Q., Tong, J-H., Zhu, Y-S. and Chen, G-Q. 2003, Leukemia, 17, 2065-2073.
9. Ching-Yuan, W., Hong-Yo, K., Wei-Lei Y., Juan W., Yun Seong, J., Jing, W., Chia-Hsin, Ch., Szu-Wei, L., Xian, Z., Lamothe, B., Campos, A. D., Darnay, B. G. and Hui-Kuan L. 2011, Journal of Biological Chemistry, 286, 30806–30815.

10. Mao, Z., Bozzella, M., Seluanov, A. and Gorbunova, V. 2008, DNA Repair, 7, 1765–1771.
11. Scully, R. and Xie, A. 2013, Mutation Research – Fundamental and Molecular Mechanisms of Mutagenesis Journal, 750, 5–14.
12. Rogakou, E. P., Pilch, D. R., Orr, A. H., Ivanova, V. S. and Bonner, W. M. 1998, Journal of Biological Chemistry, 273, 5858–5868.
13. Huang, X., Halicka, H. D., Traganos, F., Tanaka, T., Kurose, A. and Darzynkiewicz, Z. 2005, Cell Proliferation Journal, 38, 223–243.
14. MacPhail, S. H., Banáth, J. P., Yu, Y., Chu, E. and Olive, P. L. 2003, Journal of Radiation Research, 159, 759–767.
15. Tanaka, T., Halicka, H. D., Huang, X., Traganos, F. and Darzynkiewicz, Z. 2006, Cell Cycle, 5, 1940–1945.
16. Huang, X., Tanaka, T., Kurose, A., Traganos, F. and Darzynkiewicz, Z. 2006, International Journal of Oncology, 29, 495–501.
17. McManus, K. J. and Hendzel, M. J. 2005, Molecular Biology of the Cell, 16, 5013–5025.
18. Ichijima, Y., Sakasai, R., Okita, N., Asahina, K., Mizutani, S. and Teraoka, H. 2005, Biochemical and Biophysical Research Communications, 336, 807–812.
19. Zhao, B., Rothenberg, E., Ramsden, D. A. and Lieber, M. R. 2020, Nature Reviews Molecular Cell Biology, 21, 765–781.
20. Gell, D. and Jackson, S. P. 1999, Nucleic Acids Research, 27, 3494–3502.
21. Woods, D. S., Sears, C. R. and Turchi, J. J. 2015, PLoS ONE, 10, e0127321.
22. Jette, N. and Lees-Miller, S. P. 2015, Progress in Biophysics and Molecular Biology, 117, 194–205.
23. Kapałczyńska, M., Kolenda, T., Przybyła, W., Zajączkowska, M., Teresiak, A., Filas, V., Ibbs, M., Bliźniak, R., Łuczewski, Ł. and Lamperska, K. 2018, Archives of Medical Science, 14(4), 910-919.
24. Eaton, S. L., Roche, S. L., Hurtado, M. L., Oldknow, K. J., Farquharson, C., Gillingwater, T. H. and Wishart, T. M. 2013, PLoS One, 8(8), e72457.
25. Zellner, M., Babeluk, R., Diestinger, M., Pirchegger, P., Skeledzic, S. and Oehler, R. 2008, Electrophoresis, 29(17), 3621-7.